Chapter-III

Energy Storage Properties of cold sintered $Ba_{0.7}Sr_{0.3}TiO_3$ /PVDF Polymer Ceramic Nanocomposites

3.1 Introduction

As discussed in chapter I, there is a high demand of energy storage devices that have high temperature stability, high discharge efficiency, high energy storage density, low dielectric loss, small in size and environment friendly, for many applications such as aerospace engineering, transportation, dielectric capacitors etc.[136]. Energy storage in dielectric capacitors is a more feasible, exciting and alternate method to store and deliver high power in comparison to the electrochemical super-capacitors. Discharge efficiency of a dielectric can be calculated quantitatively with the help of polarization (P)-electric field (E) hysteresis loop which is defined as the ratio of area under the hysteresis curve between polarization axis for discharging cycle and area under the hysteresis curve between polarization axis for charging cycle. If the curves corresponding to forward and reverse cycle (charging and discharging cycle) are different that means the total energy delivered to the capacitor can't be recovered from the capacitor. This energy difference is known as dielectric loss of the capacitor material[2].

The energy storage characteristics in dielectric materials like polymer-based ferroelectrics [2,137], glass-ceramics [138] and relaxer-ferroelectrics [139] are widely studied till now. Among these dielectrics, polymer-based ferroelectrics have their own importance due to extremely high dielectric breakdown strength and lower synthesis temperature [140]. In general, PVDF exhibits four crystalline phases, namely α, β, γ and δ out of which α is non-polar while β (polar form of α or γ at high electric field ~ 5MV/m), γ and δ are polar ferroelectrics [141–143]. In various ceramic ferroelectrics, perovskite-based ferroelectrics are mostly used because of their low leakage current and high dielectric constant. Among various perovskite-based ferroelectrics, the Barium Titanate based ferroelectrics are most widely used because of its high dielectric permittivity with low dielectric loss characteristics[144–146]. Further, Barium Strontium Titanate (BST) has attracted great

attention of researchers due to its high dielectric permittivity up to 5000, thermal stability and field tunable ability. BST has been used in various applications like piezoelectric transducers, positive temperature coefficient (PTC) thermistors, pyroelectric sensors, ferroelectric memories, tunable oscillators and dielectric capacitors because of its low leakage current, good thermal stability, high dielectric constant with better piezoelectric, pyroelectric, relaxor ferroelectric properties [144–146].

A material can be suitable for large energy storage applications which has relatively high dielectric constant, high dielectric breakdown strength and low dielectric loss[147]. Polymers exhibits low dielectric constant (<20) and high dielectric strength value whereas ceramic materials have high dielectric constant but the lower value of dielectric strength[148]. Both have certain limitations in some applications where high energy storage density is required. Researchers are looking for the possibility to create a composite material made up of ceramics and polymers that can have a comparatively high dielectric breakdown strength, high dielectric constant and suitability to use in high energy density applications[130,149,150]. To fulfill these requirements, many composite films were synthesized using ceramic fillers dispersed in different polymer matrices but this scheme has the limitation on volume fraction of the filler which can be added up to the percolation limit only. Percolation happens when randomly dispersed ceramic particles in a polymer matrix start getting interconnected at a critical volume fraction [130,149,150]. The ceramic particles dispersed in the polymer matrix above percolation limit have particle-particle contacts which highly affects the desired dielectric properties and mechanical strength of the composite. To avoid the percolation problem, polymer- ceramic composites were prepared using the ceramic material as the matrix and polymer as the filler [150–153]. However, the ceramics need much higher sintering temperatures.

Several properties like electrical conductivity, dielectric permittivity, mechanical strength and dielectric breakdown strength are highly dependent on the density of the ceramic dielectric material. Sintering is a process that converts particles into compact form through competitive processes of coarsening and densification which results in the minimization of surface free energy[131,149,154,155]. The traditional sintering of ceramics is performed generally at a high temperature which is energy-consuming and not appropriate for polymers with relatively much lower degradation temperature. The chemical stoichiometry of the resulting product may change in case of volatile elements or co-firing of different materials, resulting in the deterioration of properties and crystal structure due to the creation of defects. Co–sintering of ceramics and polymer composite in one step with ceramic as a matrix looks very difficult task due to the huge difference in typical sintering temperatures of ceramics and lower polymer degradation temperatures[127–129]. This difficulty can be circumvented by introducing a newly invented sintering technique which is known as the cold sintering process[127–129,132].

The properties of a good dielectric capacitor with high recoverable energy density and high discharge efficiency are as follows: High dielectric breakdown strength, large saturation polarization, small remnant polarization, low loss tangent, and better temperature stability[156,157]. Sufficient literature is available on polymer-ceramic composite films using a polymer as a matrix for high energy density capacitor application but there are some drawbacks of the composites in film form. The ceramics cannot be dispersed above percolation limit. Due to the percolation problem, only a limited amount of ceramic filler can be loaded in the polymer matrix.

In the present study, $Ba_{0.7}Sr_{0.3}TiO_3$ (BST) nanoparticles have been synthesized using the sol-gel combustion method and its composite with PVDF polymer (80 wt.% BST – 20 wt.% PVDF) having ceramic as the matrix and polymer as filler have been prepared using

cold sintering process as described in Chapter 2. Structural, thermal stability, microstructural, dielectric, P-E characteristics and Weibull analysis have been performed to study the energy storage behavior of developed Polymer- ceramic composites. The results of this chapter are published in Journal of Materials Science: Materials in Electronics 34 (2023) 1939.

3.2 Synthesis of $Ba_{0.7}Sr_{0.3}TiO_3$/PVDF nanocomposites

Barium Strontium Titanate ceramic powder was prepared by Sol-gel combustion method. In this process, Stoichiometric amount of Barium Nitrate ($Ba(NO_3)_2$, LOBA Chemie, 99%), Strontium Carbonate ($SrCO_3$, Sigma Aldrich, 98 %), Titanium Isopropoxide ($C_{12}H_{28}O_4Ti$, Sigma Aldrich >97%) were used as the primary reagents for Ba (II), Sr(II), Ti(IV) respectively. Citric acid monohydrate ($C_6H_8O_7.H_2O$, Qualikems > 97%) was used as the fuel. Distilled water and Ethanol (C_2H_5OH, 99.9% by vol.) were used as the solvent. Ammonia solution (GSC, 25% NH_3) was used to control the pH of the solution. Strontium nitrate was prepared by dissolving strontium carbonate in dilute nitric acid. Barium Nitrate, strontium nitrate and citric acid were dissolved in separate beakers with 50 ml distilled water each. All the three solutions were mixed and kept for continuous stirring at 120 ºC on hot plate. Titanium isopropoxide (TTIP) solution was stabilized in Ethanol by adding drop by drop of TTIP in 50 ml of Ethanol. This stabilized solution of TTIP was added drop by drop in the solution of other reactants on hot plate and then ammonia solution was added to maintain the pH of the solution around 7. After continuous stirring at 120 ºC for 24h - 48 h, above solution converted into gel form which was dried at 150 ºC. This precursor powder was calcined at 750 ºC in order to obtain single phase BST solid solution. A schematic diagram of the synthesis procedure is illustrated in Fig. 3.1. Disc shaped pellets of ceramic were prepared by using 2 % water solution of PVA as binder with uniaxial

hydraulic press at optimized load of 60 kN/cm^2. The pellets were conventionally sintered at 1250 ºC and density was measured by Archimedes principle.

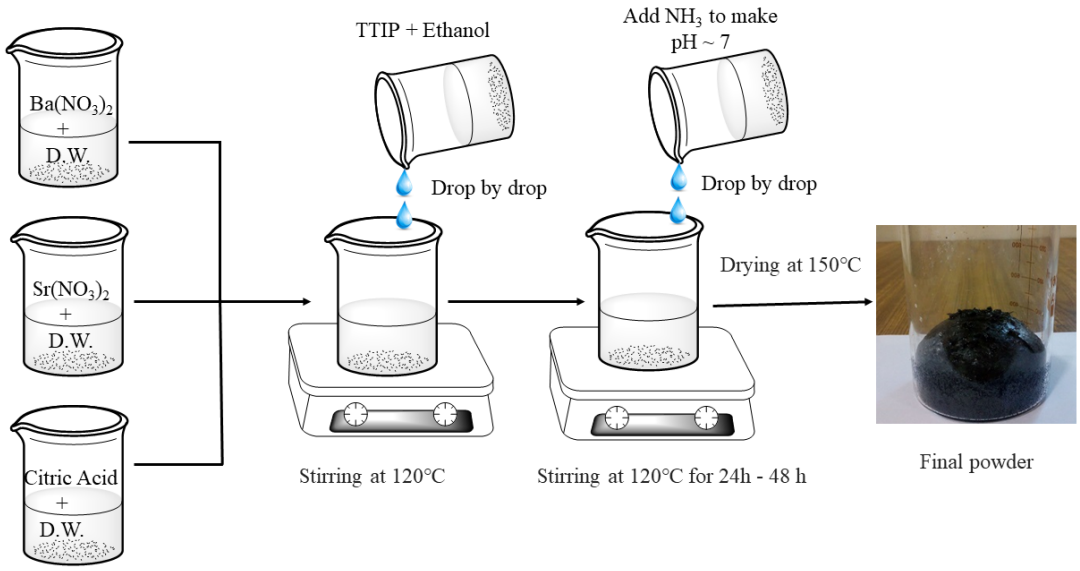

Fig. 3.1 Schematics for synthesis of BST via Sol- gel combustion process

The BST/PVDF composite was prepared using BST ceramic powder calcined at 750 ºC and PVDF polymer adopting recently devised cold sintering process. The 80 wt.% of BST and 20 wt.% of PVDF were mixed together using mortar pestle by adding some drop of distilled water as a medium for 20-30 min. After that the mixed powder was transferred into a uniaxial die of 15 mm diameter and pressed at 170 ºC and 500 MPa pressure for 15 minutes to obtain cold sintered composite pellet. The cold sintered composite pellets were prepared by using hydraulic press (Metrex Scientific Instruments Private Limited, Model No MHP-12) with heated jacket. The cold sintered composite was then annealed at 300 ºC for 1 hr and its properties have been studied. The flow chart of the cold sintering process is shown in Fig. 3.2.

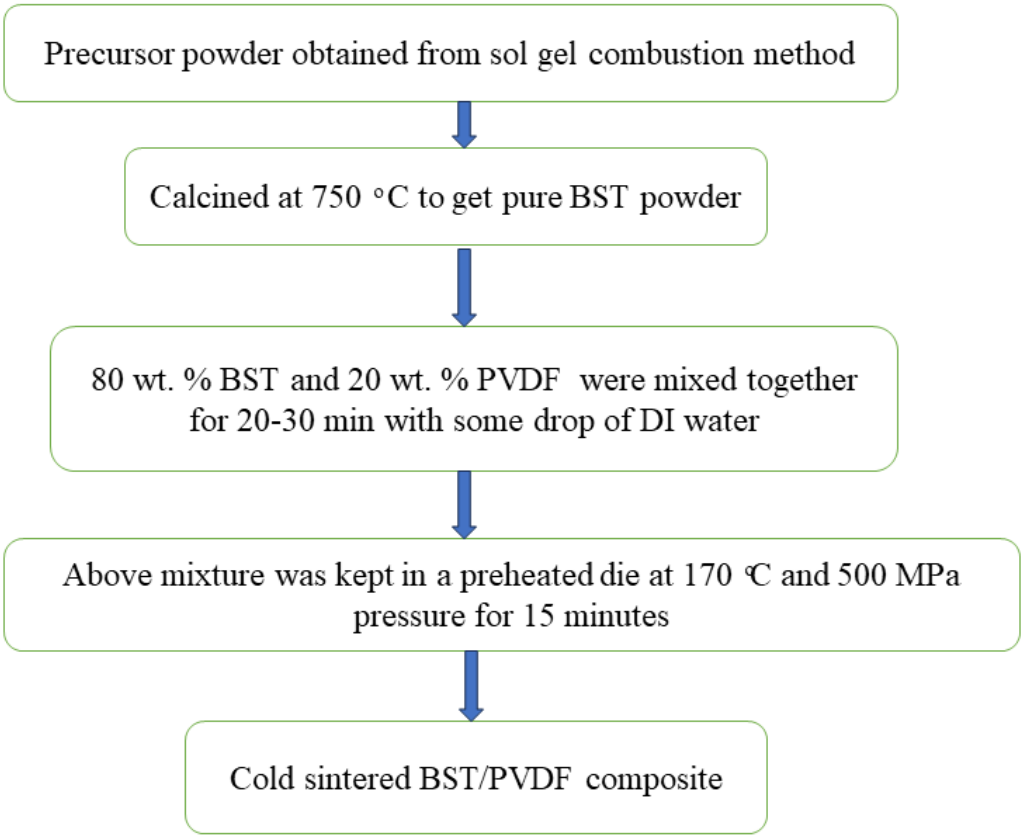

Fig. 3.2 Flow chart describing BST/PVDF composite using cold sintering process

3.3 Results and discussion

3.3.1 Structural Analysis

X-ray diffraction analysis of the samples have been performed to study the structural behavior. The XRD patterns of BST, BST/PVDF composite, PVDF and BST/PVDF composite annealed at 300 ºC for 1 h, are given in Fig. 3.3(a) and 3.3(b). PVDF powder used in the current research work was purchased directly from Alfa Aesar. The acquired PVDF powder originally consists of the α-phase. After hot pressing at 180-200 ºC, β- phase of PVDF crystallizes and further annealing at 300 ºC for 1 hr, the α and γ both phases co-exist as can be seen from Fig. 3.3(b) [158].

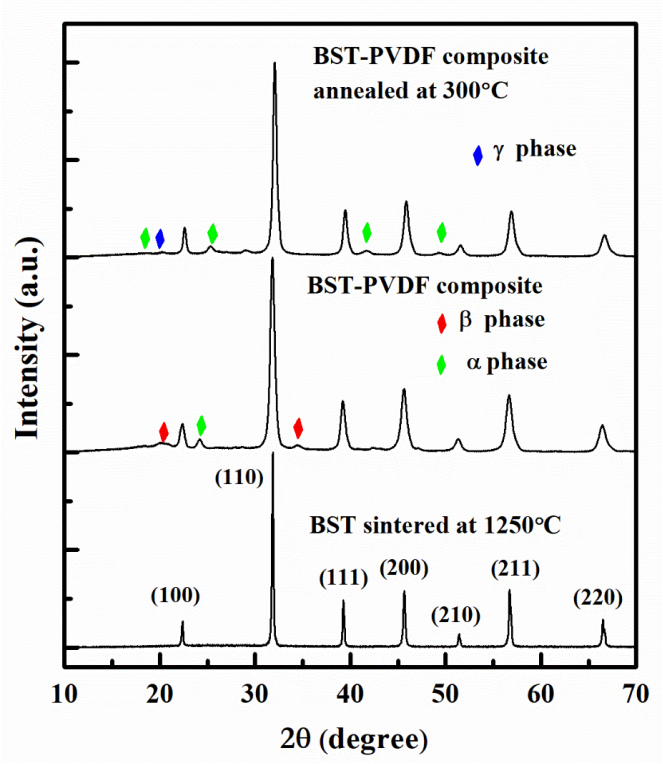

Fig. 3.3 (a) XRD patterns of BST sintered ceramic, BST/PVDF composite and BST/PVDF annealed composites

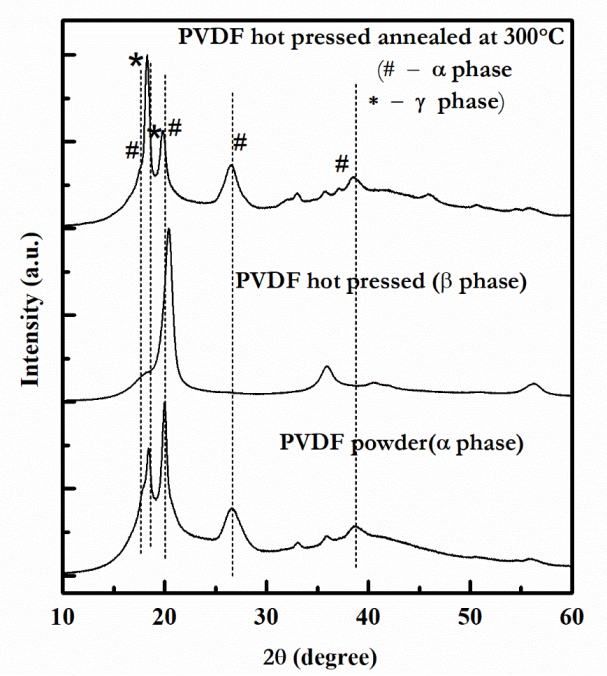

Fig. 3.3 (b) XRD patterns of PVDF powder, PVDF hot pressed and PVDF hot pressed annealed at 300 ºC.

On annealing PVDF polymer close to its melting temperature, crystallization of α and γ both phases occurs and on further increasing annealing temperature, the fraction of γ phase increases[2]**.** The XRD pattern of BST ceramic sintered at 1250 ºC, confirms that there is formation of single-phase BST with perovskite structure as shown in Fig.3(a). No other extra peak of any secondary phase was observed. The crystal structure is confirmed to be cubic with Pm-3m space group as there is no peak splitting (JCPDS ref code: 34-0411). As shown in Fig.3.3(a), the XRD patterns of BST/PVDF composites synthesized through Cold sintering process have peaks corresponding to the β-phase of PVDF as well as nanocrystalline BST. It also reveals that there is crystallization of β-phase for PVDF on hot pressing of the composite. On annealing the composites, peaks corresponding to BST and (α+γ) PVDF have been obtained that confirms that crystallization of α+γ phases have also occurred. These results on PVDF polymer are in good agreement with the results reported previously for PVDF [55,137]. Among various known phases of PVDF polymer, γ-phase has largest breakdown strength of the order of 5000 KV/cm [107]. Thus, crystallization of γ-phase is a good sign for high energy density storage application of the developed nanocomposite.

3.3.2 Density Measurement

The density of the pure BST sintered pellet and BST/PVDF composites can be determined using the formula as given below:

$$\text{Bulk density} = \frac{D}{D-S} \text{ x density of water}$$

Where D is the dry weight of the sample, S is the weight of the sample suspended in water. The density of water is 1.0 gm/cm^3.

The theoretical density of the sample can be calculated from the molecular weight of the sample and unit cell volume with the help of following formula:

$$\text{Theoretical density} = \frac{\text{n x molecular wt. of the sample}}{\text{N}*a^3}$$

Where n, N and 'a' are the number of molecule in single unit cell, Avogadro number ($6.023*10^{23}$) and lattice parameter of the sample respectively.

Density of the composites can be calculated using the rule of mixture which is given below:

$$d = d_1V_1 + d_2V_2$$

where d_1 and d_2 are the density of composite segments, V_1 and V_2 are the volume fractions of the components from which composites have been synthesized.

$$\% \text{ density} = \frac{Bulk\ density}{Theoretical\ density} \text{ x } 100$$

The bulk densities of the conventionally sintered BST at 1250 ºC, BST/PVDF composites and BST/PVDF annealed composites were quantified using Archimedes' principle. The obtained densities for these three type of samples are listed in Table 1. The density of conventionally sintered BST was found to be about 99 % of the theoretical density i.e. 5.62 g/cc. The densities of BST/PVDF composite and BST/PVDF annealed composite were found to be 3.80 g/cc and 3.68 g/cc, respectively, which is approximately 97% and 94% of the theoretically calculated value of the density. We found that the density of BST/PVDF annealed composite is slightly less than that of BST/PVDF composite due to volume expansion of β-PVDF when it transforms to α+γ- PVDF.

Table 3.1: Bulk densities of sintered BST ceramic, BST/PVDF composite and BST/PVDF annealed composite.

S. No.	**Sample Name**	**Bulk density (g/cc)**	**Relative density (%)**
1.	Sintered BST ceramic	5.62	99
2.	BST/PVDF composite	3.80	97
3.	BST/PVDF annealed composite	3.68	94

3.3.3 Thermal Analysis

Thermogravimetric analysis (TGA) and Differential Scanning Calorimetry (DSC) analysis were carried out to determine the thermal stability of the hot pressed BST/PVDF composite and the corresponding curves are shown in Fig.3.4. From Fig.3.4, we can see that there is very little weight loss in TGA curve up to 300 ºC. Above 300 ºC, sharp decrement is observed in the TGA curve between 400 ºC – 500 ºC, which represents the weight loss for PVDF polymer in the BST/PVDF composite. This result is consistent with the previously reported TGA curve for PVDF polymer. In the DSC curve of composite, an endothermic peak is observed in the same temperature range. This suggests that weight loss happens due to pyrolysis of polymeric chain which is an endothermic process and results in removal of polymers from the composite [107]. Therefore, we can conclude that the BST/PVDF composite is stable enough up to the temperature of 300 ºC.

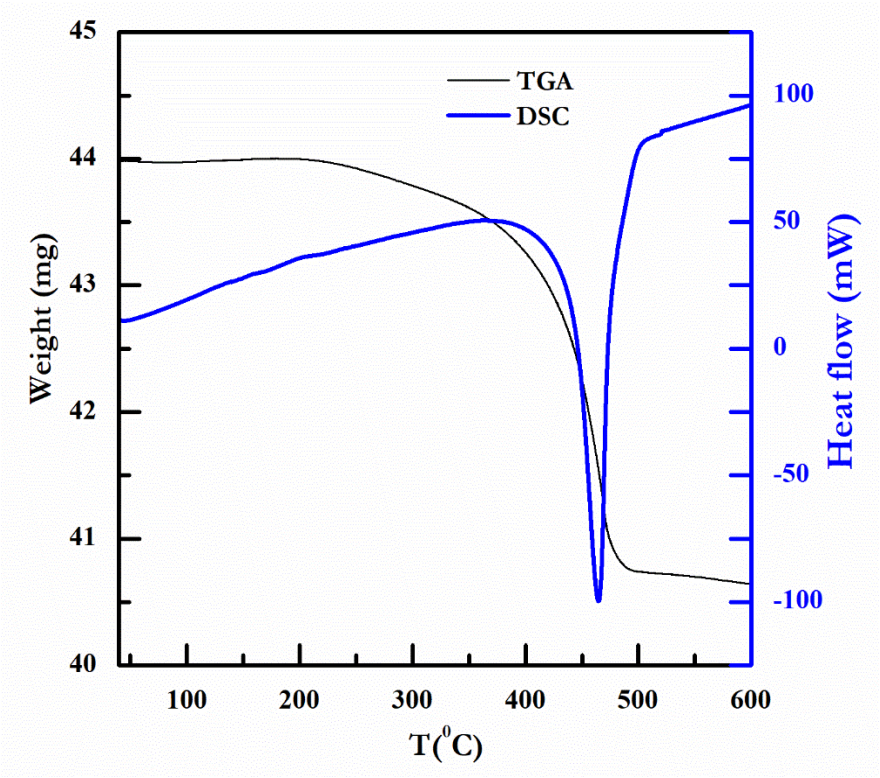

Fig. 3.4 TGA and DSC curves of BST/PVDF composite

3.3.4 Microstructural Analysis

Microstructural properties of the synthesized BST and its composite with PVDF were studied using field emission scanning electron microscope (FESEM). Fig.3.5 shows the FESEM images of conventionally sintered BST ceramic, fractured surfaces of hot pressed BST/PVDF composite and BST/PVDF annealed composite. Conventionally sintered BST shows dense microstructure without any pore. The average grain size of conventionally sintered BST was found to be 1 μm as shown in the Fig.3.5 (a). The morphology of hot pressed BST/PVDF composite and BST/PVDF annealed composite shows uniform distribution of PVDF polymer around ceramic BST grains. From the FESEM image of the fractured surface of BST composite, it can be concluded that composites are highly dense, pore-free with homogeneous distribution of PVDF polymer in BST ceramic matrix. BST ceramic grains are not clearly visible in the composite. This is attributed to the trapping of several smaller ceramic grains in molten PVDF polymer; hence its exact grain size can't be predicted. From the HR-SEM image of annealed composite, we can see some grain surfaces resolved after annealing process. A detailed investigation of evolution of morphology during cold sintering in such types of composites is a subject matter of investigation.

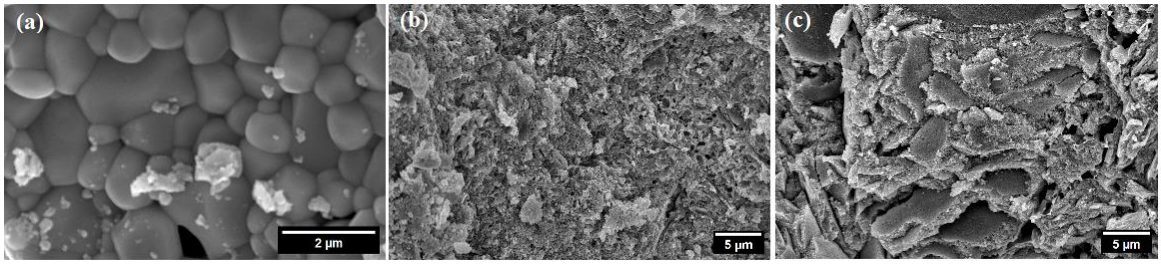

Fig.3.5 FESEM images of (a) Conventionally sintered BST ceramic (surface), (b) BST/ PVDF composite, (c) BST/PVDF composite annealed at 300 ºC for 1 hr.

Fig. 3.6 depicts the elemental mapping of the hot pressed BST/PVDF composite obtained from the energy dispersive spectroscopic (EDS) analysis. In the selected part of

the image corresponding to BST, there is high amount of Ba, Sr, and Ti distribution observed while the distribution of C and F atoms are limited to the surroundings and surfaces of ceramic grains due to the presence of PVDF polymer in the composite.

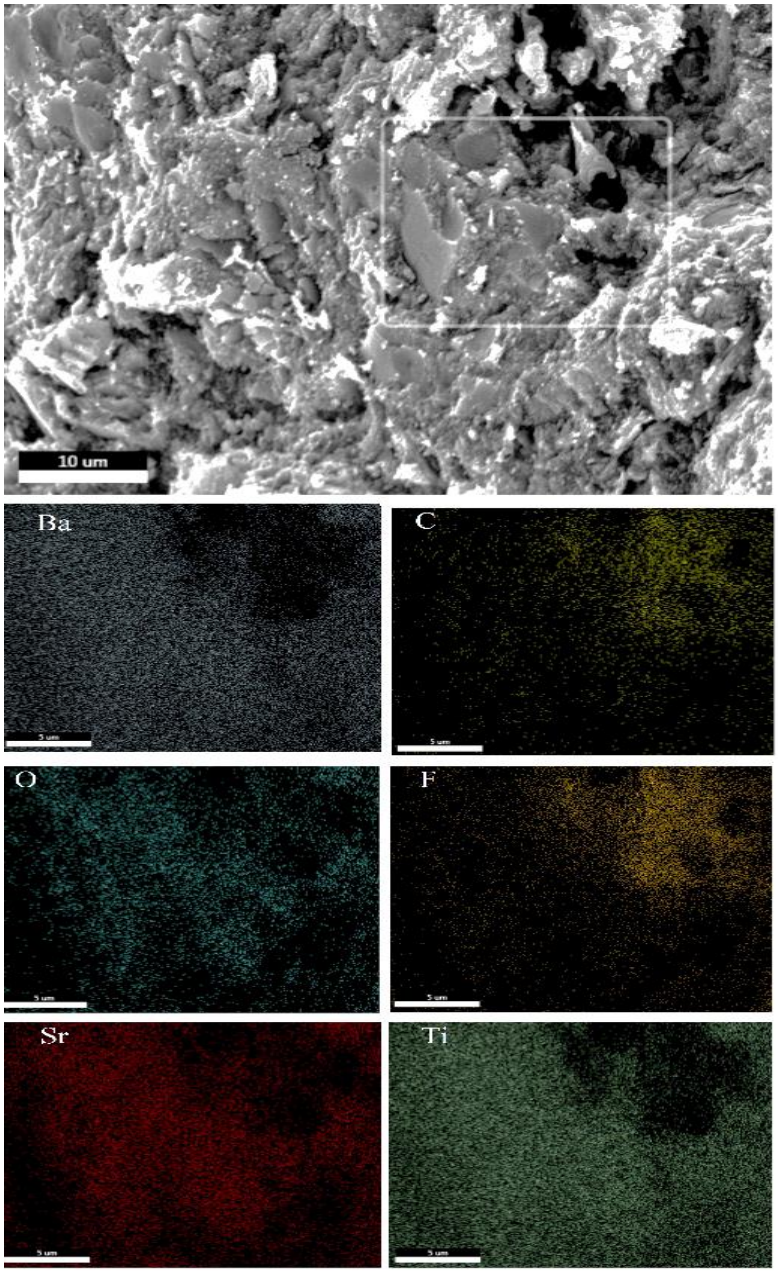

Fig.3.6 Elemental mapping of hot pressed BST/PVDF composite.

3.3.5 Dielectric Measurement

The temperature dependence of dielectric permittivity of conventionally sintered BST, hot-pressed PVDF, hot pressed BST/PVDF composite and BST/PVDF annealed composite were studied after applying silver paste electrodes on flat sides of the samples.

The temperature dependence of the permittivity and loss tangent of the conventionally sintered BST and hot-pressed PVDF samples are shown in Fig.3.7. As can be seen from Fig.3.7(a) and (b), conventionally sintered $Ba_{0.70}Sr_{0.30}TiO_3$ ceramic has high dielectric constant and low dielectric loss at room temperature since its ferroelectric tetragonal to paraelectric cubic phase transition is slightly below room temperature. From the behavior of temperature dependence of permittivity of conventionally sintered BST ceramic, it can be inferred that there is evidence of phase transition in dielectric response below room temperature and only the downfall of the peak is recorded. It is in full agreement with previously reported tetragonal P4mm to cubic Pm-3m phase transition for this composition[159]. Fig.3.7 (c) and (d) show the temperature dependence of the permittivity and loss tangent of the hot-pressed PVDF samples. It can be seen from the figure, that the dielectric permittivity of hot pressed PVDF increases but dielectric loss decreases with decreasing frequency at room temperature. A broad peak in the temperature dependence of permittivity around 130 ºC might be due to the α relaxation behaviour of PVDF. The dielectric properties of hot pressed PVDF and annealed hot pressed PVDF polymer has been already reported in literature [107]. Our result is in good agreement with the reported data on the hot-pressed PVDF sample. In the case of annealed hot pressed PVDF sample, the same pattern is observed with some increasing value of dielectric constant and decreasing value of dielectric loss at room temperature which confirms the crystallization of γ-phase improves the dielectric properties of PVDF hot pressed sample [107,157,160].

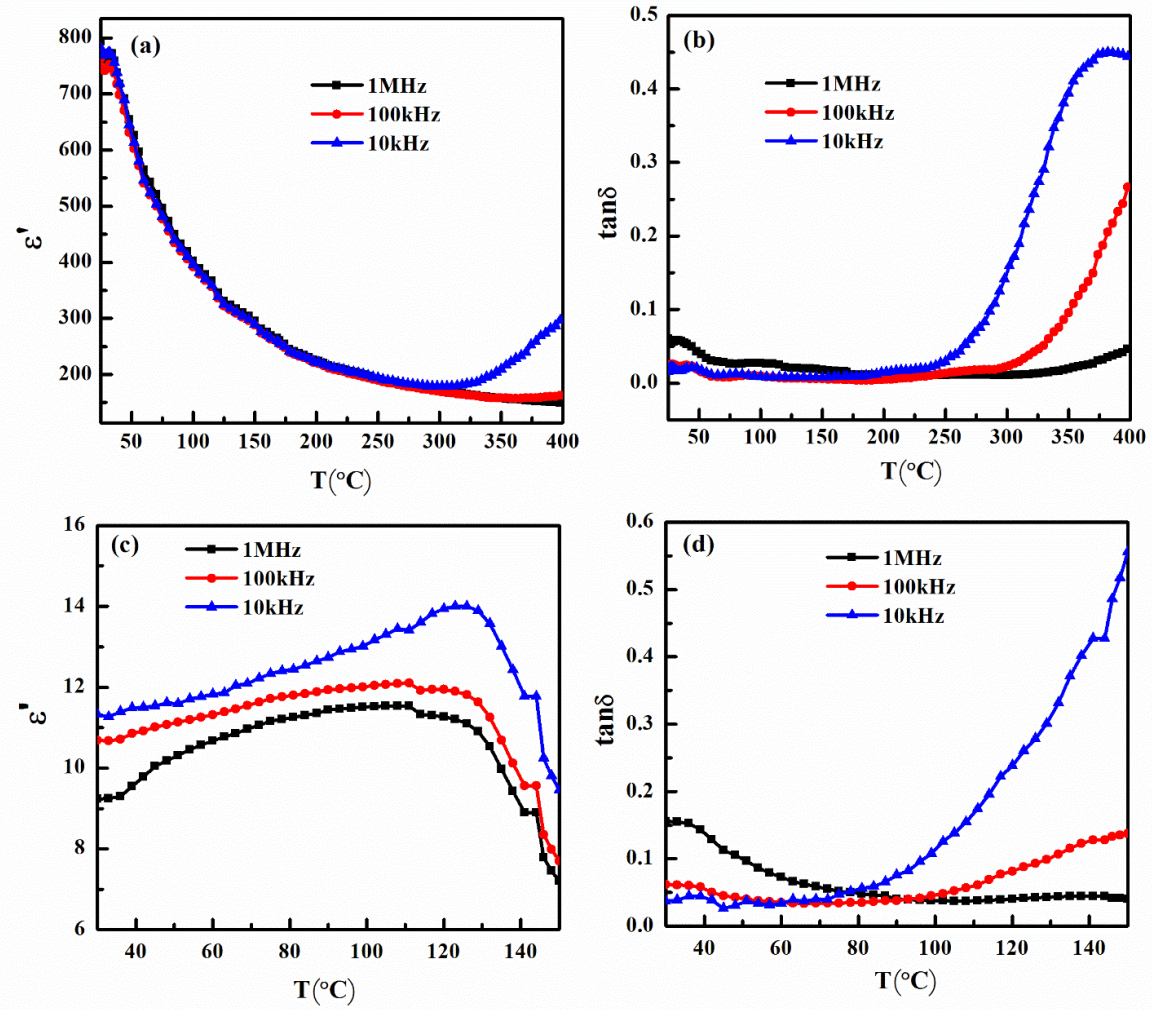

Fig. 3.7 (a) Dielectric constant, (b) Loss tangent of BST sintered ceramic and (c) Dielectric constant, (d) Loss tangent of PVDF hot pressed.

Fig.3.8 shows the temperature dependence of the permittivity and loss tangent of the hot pressed BST/PVDF composite and BST/PVDF annealed composite. In case of composites, the value of dielectric constant is found to be moderate and in between that of BST ceramic and PVDF polymer. The BST/PVDF annealed composite has sightly low value of dielectric constant and loss tangent with better frequency stability in comparison to hot pressed BST/PVDF composite as can be seen from Fig.3.8 (b), (d). Around the temperature range 100 ºC, a weak dielectric transition is visible in the composite similar to hot pressed PVDF, therefore it can be attributed to the α-relaxation in PVDF polymer [161]. A comparison of the dielectric behaviour of hot pressed BST/PVDF composite and annealed composite reveals

that this transition temperature shifts towards lower temperature side after annealing. Dielectric constant of BST/PVDF annealed composite has better thermal stability and the dielectric loss is also significantly reduced which makes it more suitable for energy storage material. The temperature variation in dielectric constant is negligible and the value of loss tangent is less than 0.3 in the case of annealed composite up to 200 ºC temperature which predicts that the composite has better thermal stability in this temperature range. PVDF polymer starts softening/melting above 165 ºC and hence it can lead to aggregation of molten polymer around the grain boundary areas which become more prominent above 200 ºC. The presence of semi-crystalline PVDF polymer around the grain boundary areas of ceramics enhances the resistivity at grain boundaries which creates a space charge polarization effect leading to high dielectric constant and loss tangent along with high-frequency dependence. After this temperature range, the pyrolysis of the polymer may start that can lead to an enormous increase in loss tangent along with dielectric constant. In Table 3.2, we have given comparison of the dielectric permittivity of previously reported BST based different polymer composites with our sample. The composite sample developed by us has the best response among all these systems.

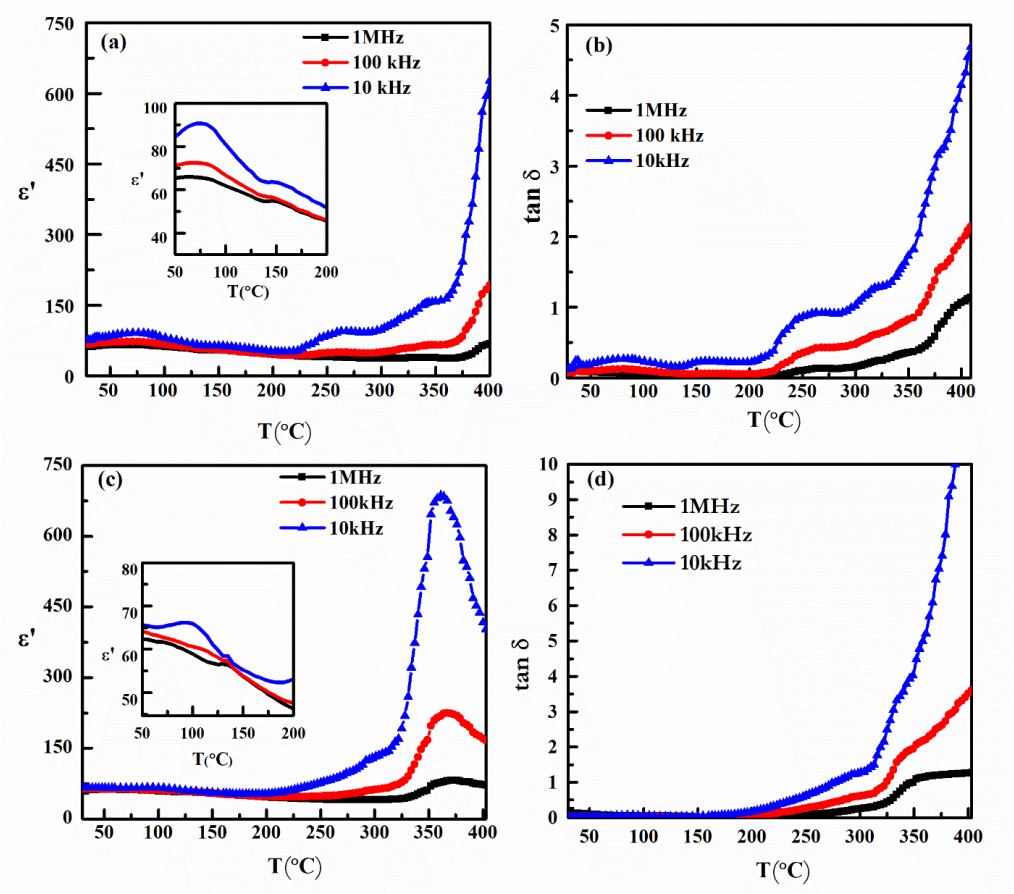

Fig. 3.8 Temperature dependence of dielectric constant of (a) BST/PVDF hot pressed composite, (c) BST/PVDF annealed composite and Loss tangent of (b) BST/PVDF composite, (d) BST/PVDF annealed composite.

Table 3.2: A comparison of the dielectric permittivity of different BST/Polymer Composites.

Sample Name	**Volume % of BST**	**Dielectric permittivity**	**Reference**
$Ba_{0.7}Sr_{0.3}TiO_3$/HDPE	40	12.7	[162]
$Ba_{0.6}Sr_{0.4}TiO_3$/PMMA	50	28	[163]
$Ba_{0.7}Sr_{0.3}TiO_3$/BR	39	13.1	[164]
$Ba_{0.55}Sr_{0.45}TiO_3$/PPS	36.4	14.2	[165]
BST/ER	50.5	28.5	[166]
BST/COC	45.8	13.8	[167]
$Ba_{0.7}Sr_{0.3}TiO_3$/PVDF	54.8	65	**Present work**

3.3.6 P-E hysteresis Analysis

Fig. 3.9 shows the polarization (P)-electric field (E) hysteresis loop analysis of conventionally sintered BST, hot pressed BST/PVDF composite and annealed BST/PVDF composite samples. Measurements were performed at room temperature with bipolar triangular signal of 100 Hz frequency. Fig. 3.9(a) represents the P-E hysteresis loop corresponding to BST sintered ceramic which displays a typical relaxor type ferroelectric loop with remnant polarization of about 1 $\mu C/cm^2$, coercive field ~ 20 kV/cm, breakdown field about more than 125 kV/cm, and some hysteresis loss. It is well known that relaxor ferroelectrics show slim P-E hysteresis loop even in centrosymmetric cubic structure. The P-E hysteresis loop for hot pressed BST/PVDF composite shows relatively less remanent polarization of 0.25 $\mu C/cm^2$ but increased loss and coercive field as shown in Fig. 3.9 (b). The β-crystalline phase of PVDF polymer is also ferroelectric in nature with lossy hysteresis loop indicating that it is not much suitable for energy storage applications[107]. Comparatively, the hysteresis loop of annealed BST/PVDF composite showed little hysteresis loss and remnant polarization with no dielectric breakdown even when an electric field of 400 kV/cm was applied, up to the measured field limit of the instrument used. Thus, the introduction of PVDF polymer filler to the ceramic matrix boosted electrical breakdown strength in such a way that it did not get breakdown even after applying four times higher electric field than what single phase BST ceramic can withstand. Dielectric breakdown in ceramics is a result of spatial fluctuations of the local field. The existence of a polymeric phase among the ceramic grains can cause hindrance in the interaction of this local field around grain interfaces when the external field is applied. Thus, the dielectric breakdown strength of BST ceramic is enhanced significantly on the introduction of PVDF polymeric phase in composite. The values of remnant polarization (P_r), maximum polarization (P_m), energy storage density (U_e) and discharge efficiency **(**η) for pure BST,

hot pressed BST/PVDF composite and annealed BST/PVDF composite are listed in Table 3.3. The discharge efficiency in case of annealed BST/PVDF composite is found to be 95%, which is much better than the hot pressed BST/PVDF composite i.e., 61%.

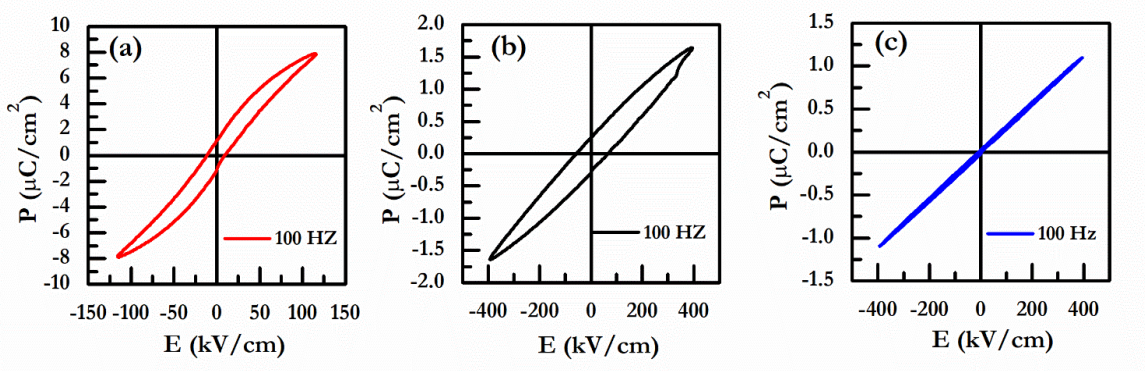

Fig. 3.9 P-E loop for (a) sintered BST ceramic, (b) hot pressed BST/PVDF composite (c) BST/PVDF composite annealed at 300 ºC for 1 hr.

Table 3.3: Remnant Polarization (P_r) , Maximum Polarization (P_m), Energy storage density (U_e) and discharge efficiency (η) of Pure BST, BST/PVDF composite and BST/PVDF annealed composite.

S. No.	Sample Name	Remnant Polarization P_r (μC/cm²)	Maximum Polarization P_m (μC/cm²)	Energy Storage density U_e (J/cm³)	Discharge efficiency η (%)
1.	Pure BST	1	8	0.465	65
2.	BST/PVDF composite	0.25	1.5	0.397	61
3.	BST/PVDF annealed composite	0.05	1	0.219	95

The energy density and discharge efficiency of the BST, hot pressed BST/PVDF composite and annealed BST/PVDF composite have been determined using the partial P-E hysteresis loop response shown in Fig.3.10-3.12. The Eq (3.1) and (3.2) given below has been used for the calculation of the energy density and energy discharge efficiency.

Recoverable energy storage density (W_{rec}) = $\int_{P_r}^{P_m} EdP$ (3.1)

Energy discharge efficiency (η) = $\frac{W_{rec}}{W_t}$ (3.2)

Where W_{rec} is the recoverable energy storage density, W_t is the total energy storage density, E is the applied electric field, P is the polarization, P_m is the maximum polarization and P_r is remnant polarization. A comparison of the energy storage density and energy discharge efficiency for BST ceramic, hot pressed BST/PVDF composite and BST/PVDF annealed composite is shown in Fig. 3.13. Highest energy discharge efficiency is obtained for the BST/PVDF annealed composite.

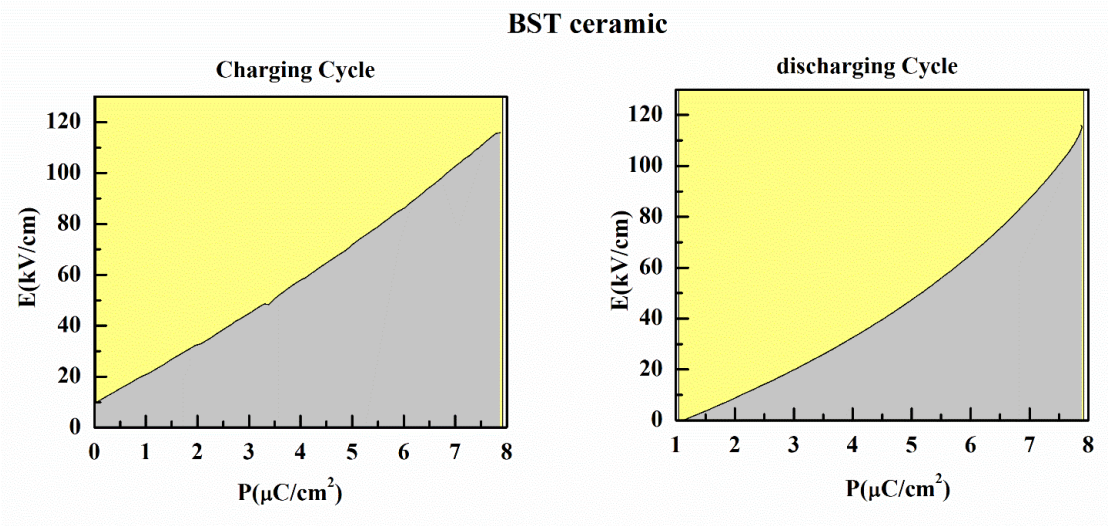

Fig. 3.10 Partial P-E hysteresis loop response for calculation of Energy density and discharge efficiency of pure BST ceramic.

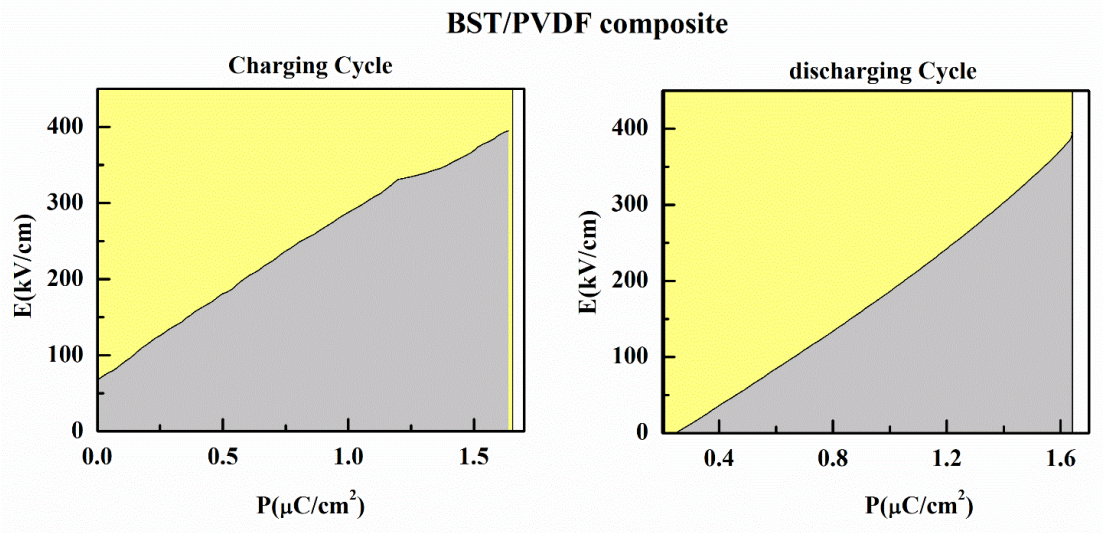

Fig. 3.11 Partial P-E hysteresis loop response for calculation of Energy density and discharge efficiency of hot pressed BST/PVDF composite.

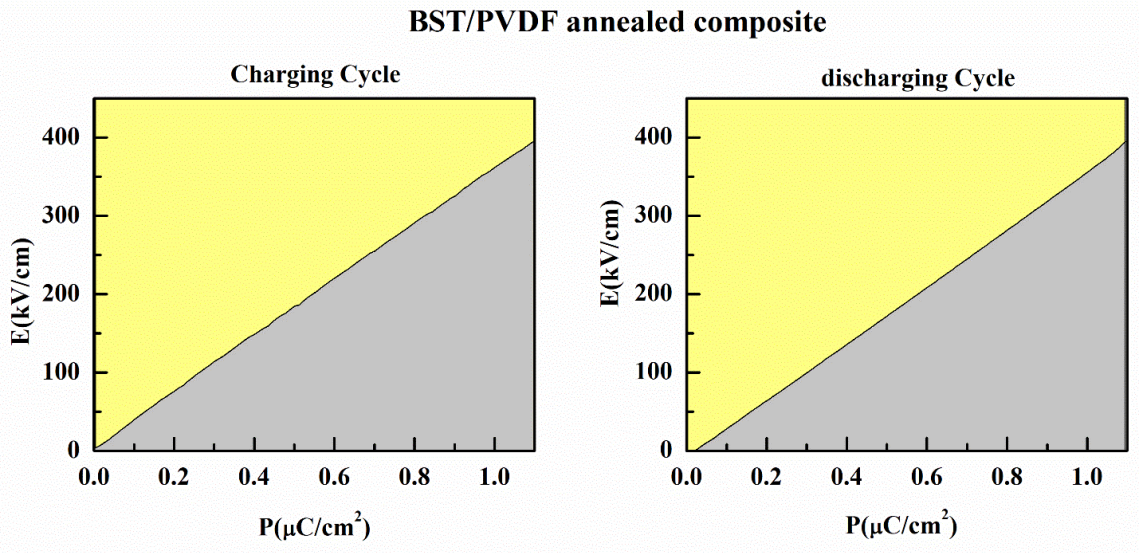

Fig. 3.12 Partial P-E hysteresis loop response for calculation of Energy density and discharge efficiency of BST/PVDF annealed composite.

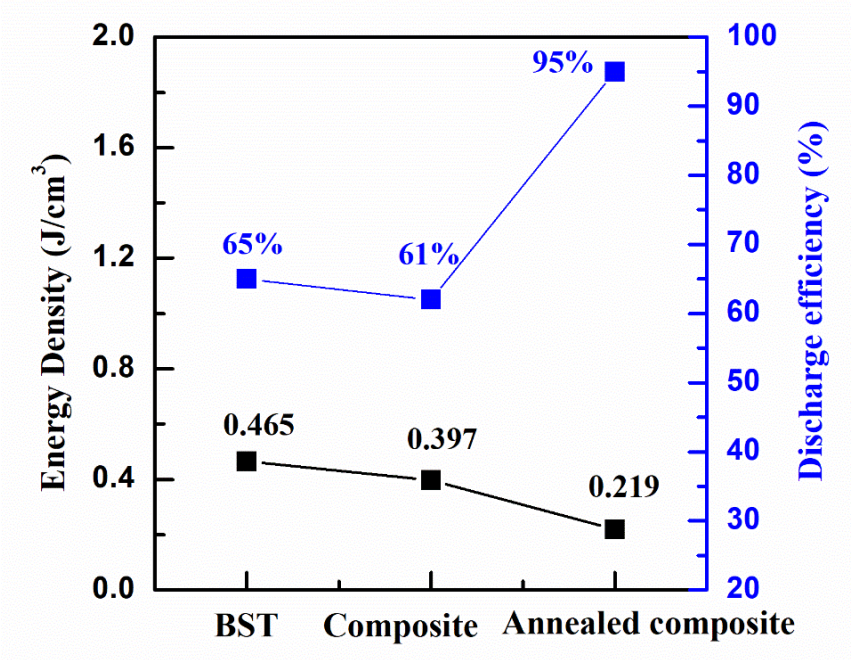

Fig. 3.13 Energy density and discharge efficiency for BST ceramic, hot pressed BST/PVDF composite and BST/PVDF annealed composite.

3.3.7 Weibull Analysis

The breakdown strength has very important role for the determination of maximum energy storage density of polymer/ceramic composites. The study of breakdown strength

of developed materials has been carried out by Weibull distribution analysis. The Weibull analysis can be performed using the below Eq. (3.3) and Eq. (3.4).

$$X_i = \ln(E_i) \tag{3.3}$$

$$Y_i = \ln(\ln\frac{1}{1-p}) \tag{3.4}$$

where X_i and Y_i represents two parameters in the Weibull distribution function, E_i is the ac breakdown voltage of i^{th} sample, n is the total number of samples in the experiments and probability of chosen sample $p = \frac{i}{(n+1)}$.

The samples are arranged in ascending order of their ac-breakdown strength value i.e., E1<E2<E3….En. The parameters Xi and Yi show linear relationship. The slope of the line gives shape parameter β and the mean value of ac-breakdown strength can be determined corresponding to the point where the linear fitting line intersect the horizontal line Y = 0. Fig 3.14 shows Weibull plots of dielectric breakdown strength of BST/PVDF annealed composite. As can be seen from this figure, cold sintering of BST ceramics with PVDF introduces a unique approach to enhance dielectric breakdown strength. The process promotes improved interfacial bonding, reducing microstructural defects and domain-related vulnerabilities, while PVDF's flexible nature may mitigate crystal anisotropy effects. It is clear from Fig. 3.14 that the Weibull plot shows good linearity and the value of shape parameter β is around 11 and the mean value of ac breakdown strength is 250 kV/cm in case of BST/PVDF annealed composite. The breakdown strength of the composite is expected to be in between the breakdown strength of the ceramic and polymer.

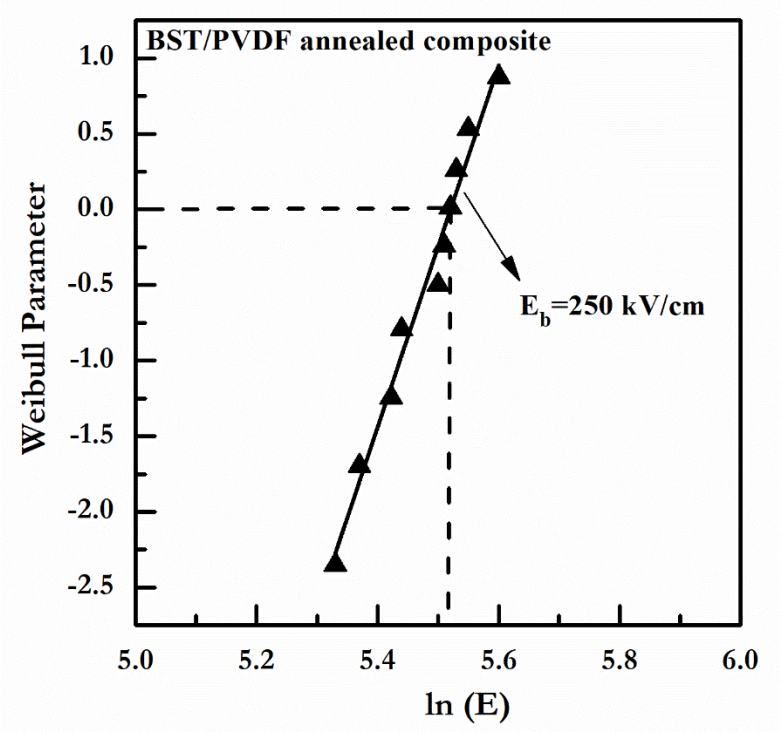

Fig.3.14 Weibull plot of dielectric breakdown strength for BST/PVDF annealed composite.

There is increment in the value of dielectric breakdown strength of ceramic when we introduce the amount of PVDF polymer filler. This can be explained in the following way. When the two materials which have much difference in the value of dielectric constant, are mixed together and they are subjected to electric field then a highly non-homogeneous electric field is generated due to huge difference of dielectric constant between polymer and ceramics [168]**.** The electric field around the polymer will be high than the mean value of electric field that leads to the reduction in the value of dielectric breakdown strength of polymer-ceramic composite in comparison to polymer but higher than the ceramic.

3.4 Conclusion:

The BST/PVDF composites with 80 wt.% BST and 20 wt.% PVDF have been synthesized by the cold sintering technique. XRD pattern confirms the formation of pure perovskite phase of BST with cubic structure having Pm-3m space group. In case of hot pressed BST/PVDF composite, crystallization of β phase and in case of annealed

BST/PVDF composite, crystallization of γ-phase dominates. TGA/DSC analysis reveals that composite is stable for the application up to 300 ºC. Thermally stable dielectric constant and dielectric loss is obtained from room temperature to 200 ºC in case of annealed BST/PVDF composite. Dielectric breakdown strength of the composite has been significantly enhanced in comparison to BST ceramic. We have achieved up to 95 % discharge efficiency in case of BST/PVDF annealed composite which is big achievement for a ceramic matrix composite with polymer filler for energy storage applications.